Squeezed quadrature fluctuations in a gravitational wave detector using squeezed light

S. Dwyer,[*1] **L. Barsotti,**[1] **S. S. Y. Chua,**[2] **M. Evans,**[1] **M. Factourovich,** [3]
D. Gustafson,[4] **T. Isogai,**[1] **K. Kawabe,**[5] **A. Khalaidovski,**[6] **P. K. Lam,**[2]
M. Landry,[5] **N. Mavalvala,**[1] **D. E. McClelland,**[2] **G. D. Meadors,**[4] **C. M.
Mow-Lowry,**[2] **R. Schnabel,**[6] **R. M. S. Schofield,**[7] **N. Smith-Lefebvre,**[1]
M. Stefszky,[2] **C. Vorvick,**[5] **and D. Sigg**[5]

[1] *LIGO - Massachusetts Institute of Technology, Cambridge, MA 02139, USA*
[2] *Australian National University, Canberra, ACT 0200, Australia*
[3] *Columbia University, New York, NY 10027, USA*
[4] *University of Michigan, Ann Arbor, MI 48109, USA*
[5] *LIGO - Hanford Observatory, Richland, WA 99352, USA*
[6] *Albert-Einstein-Institut, Leibniz Universität Hannover, Max-Planck-Institut fur
Gravitationsphysik, D-30167 Hannover, Germany*
[7] *University of Oregon, Eugene, OR 97403, USA*

*sheila.dwyer@ligo.org

Abstract: Squeezed states of light are an important tool for optical measurements below the shot noise limit and for optical realizations of quantum information systems. Recently, squeezed vacuum states were deployed to enhance the shot noise limited performance of gravitational wave detectors. In most practical implementations of squeezing enhancement, relative fluctuations between the squeezed quadrature angle and the measured quadrature (sometimes called squeezing angle jitter or phase noise) are one limit to the noise reduction that can be achieved. We present calculations of several effects that lead to quadrature fluctuations, and use these estimates to account for the observed quadrature fluctuations in a LIGO gravitational wave detector. We discuss the implications of this work for quantum enhanced advanced detectors and even more sensitive third generation detectors.

References and links

1. The LIGO Scientific Collaboration, "LIGO: The laser interferometer gravitational-wave observatory," Rep. Prog. Phys. **72**, 076901 (2009).
2. C. M. Caves, "Quantum-mechanical noise in an interferometer," Phys. Rev. D **23**, 1693 (1981).
3. R. Schnabel, N. Mavalvala, D.E. McClelland, and P.K. Lam, "Quantum metrology for gravitational wave astronomy," Nat. Commun. **1**, 121. (2010).
4. D.E. McClelland, N. Mavalvala, Y. Chen, and R. Schnabel, "Advanced interferometry, quantum optics and optomechanics in gravitational wave detectors," Laser and Photonics Rev.**5**, 677-696 (2011).
5. LIGO Scientific Collaboration, "Enhanced sensitivity of the LIGO gravitational wave detector by using squeezed states of light," Nature Photon. doi:10.1038/nphoton.2013.177 (2013).

6. LIGO Scientific Collaboration, "A gravitational wave observatory operating beyond the quantum shot-noise limit," Nature Phys. **7** (12) 962-965 (2011).
7. H Grote, K Danzmann, K Dooley, R Schnabel, J Slutsky, and H Vahlbruch, "First long-term application of squeezed states of light in a gravitational-wave observatory," Phys. Rev. Lett. **1**10, 181101 (2013).
8. K. Wódkiewicz and M. S. Zubairy, "Effect of laser fluctuations on squeezed states in a degenerate parametric amplifier," Phys. Rev. A **27**, 2003–2007 (1983).
9. D. D. Crouch and S. L. Braunstein, "Limitations to squeezing in a parametric amplifier due to pump quantum fluctuations," Phys. Rev. A **38**, 4696–4711 (1988).
10. P. K. Lam, T. C. Ralph, B. C. Buchler, D. E. McClelland, H. A. Bachor, and J. Gao, "Optimization and transfer of vacuum squeezing from a below threshold optical parametric oscillator," J. Opt. B: Quantum S. O.**1**, 469-474 (1999).
11. M. S. Stefszky, C. M. Mow-Lowry, S. S. Y. Chua, D. A. Shaddock, B. C. Buchler, H. Vahlbruch, A. Khalaidovski, R. Schnabel, P. K. Lam, and D. E. McClelland, "Balanced homodyne detection of optical quantum states at audio-band frequencies and below," Class. Quant. Grav.**29**, 145015-145029. (2012).
12. T. Eberle, S. Steinlechner, J. Bauchrowitz, V. Händchen, H. Vahlbruch, M. Mehment, H. Müller-Ebhardt, and R. Schnabel, "Quantum enhancement of the zero-area sagnac interferometer topology for gravitational wave detection," Phys. Rev. Lett. **104**, 25, 251102 (2010).
13. T. Aoki, G. Takahashi, and A. Furasawa, "Squeezing at 946 nm with periodically poled KTiOPO$_4$," Opt. Express **14** (15), 6930-6935 (2006).
14. Y. Takeno, M. Yukawa, H. Yonezawa, and A. Furusawa, "Observation of -9 dB quadrature squeezing with improvement of phase stability in homodyne measurement," Opt. Express **15**, 4321–4327 (2007).
15. A. Franzen, B. Hage, J. DiGuglielmo, J. Fiurásek, and R. Schnabel, "Experimental demonstration of continuous variable purification of squeezed states," Phys. Rev. Lett. **97**, 150505 (2006).
16. S. S. Y. Chua, S. Dwyer, L. Barsotti, D. Sigg, R. M. S. Schofield, V. V. Frolov, K. Kawabe, M. Evans, G. D. Meadors, M. Factourovich, R. Gustafson, C. Vorvick, M. Landry, A. Khalaidovski, M. S. Stefszky, C. M. Mow-Lowry, B. C. Buchler, D. A. Shaddock, P. K. Lam, R. Schnabel, N. Mavalvala, and D. E. McClelland, are preparing a manuscript to be called "Impact of backscattered-light in a squeezing-enhanced interferometric gravitational-wave detector,"
17. T. T. Fricke, N. D. Smith-Lefebvre, R. Abbott, R. Adhikari, K. L. Dooley, M. Evans, P. Fritschel, V. V. Frolov, K. Kawabe, J. S. Kissel, B. J. J. Slagmolen, and S. J. Waldman, "DC readout experiment in Enhanced LIGO," Class. and Quant. Grav. **29**, 065005 (2012).
18. S. Chua, M. Stefszky, C. Mow-Lowry, B. Buchler, S. Dwyer, D. Shaddock, P. K. Lam, and D. McClelland, "Backscatter tolerant squeezed light source for advanced gravitational-wave detectors," Opt. Lett. **36** (23) 4680-4682 (2011).
19. S. Chelkowski, H. Vahlbruch, K. Danzmann, and R. Schnabel, "Coherent control of broadband vacuum squeezing," Phys. Rev. A **75**, 043814 (2007).
20. H. Vahlbruch, S. Chelkowski, B. Hage, A. Franzen, K. Danzmann, and R. Schnabel, "Coherent control of vacuum squeezing in the gravitational-wave detection band," Phys. Rev. Lett. **97**, 011101 (2006).
21. K. McKenzie, N. Grosse, W. P. Bowen, S. E. Whitcomb, M. B. Gray, D. E. McClelland, and P. K. Lam, "Squeezing in the audio gravitational-wave detection band," Phys. Rev. Lett. **93**, 161105 (2004).
22. K. McKenzie, "Squeezing in the audio gravitational wave detection band," Ph.D. thesis, Australian National University (2008).
23. J. Gea-Banacloche and M. S. Zubairy, "Influence of pump-phase fluctuations on the squeezing in a degenerate parametric oscillator," Phys. Rev. A **42**, 1742–1751 (1990).
24. M. J. Collett and C. W. Gardiner, "Squeezing of intracavity and traveling-wave light fields produced in parametric amplification," Phys. Rev. A **30**, 1386–1391 (1984).
25. C. W. Gardiner and M. J. Collett, "Input and output in damped quantum systems: Quantum stochastic differential equations and the master equation," Phys. Rev. A **31**, 3761–3774 (1985).
26. K. McKenzie, M. B. Gray, P. K. Lam, and D. E. McClelland, "Nonlinear phase matching locking via optical readout," Opt. Express **14**, 11256–11264 (2006).
27. A. Khalaidovski, H. Vahlbruch, N. Lastzka, C. Gräf, K. Danzmann, H. Grote, and R. Schnabel, "Long-term stable squeezed vacuum state of light for gravitational wave detectors," Class. and Quant. Grav. **29**, 075001 (2012).
28. K. Goda, K. McKenzie, E. E. Mikhailov, P. K. Lam, D. E. McClelland, and N. Mavalvala, "Photothermal fluctuations as a fundamental limit to low-frequency squeezing in a degenerate optical parametric oscillator," Phys. Rev. A **72**, 043819 (2005).
29. G. M. Harry (for the LIGO Scientific Collaboration), "Advanced LIGO: the next generation of gravitational wave detectors," Class. Quant. Grav. **27**, 084006 (2010).
30. A Khalaidovski, "Beyond the quantum limit: A squeezed light laser in GEO600," Ph.D. thesis, Gottfried Wilhelm Leibniz Universität Hannover (2011).
31. Einstein gravitational wave telescope conceptual design study. https://tds.ego-gw.it/ql/?c=7954
32. K. McKenzie, E. E. Mikhailov, K. Goda, P. K. Lam, N. Grosse, M. B. Gray, N. Mavalvala, and D. E. McClelland, "Quantum noise locking," J. Opt. B: Quantum S. O. **7**, S421 (2005).

33. C. M. Caves and B. L. Schumaker, "New formalism for two-photon quantum optics. I. Quadrature phases and squeezed states," Phys. Rev. A **31**, 3068–3092 (1985).
34. B. Buchler, "Electro-optic control of quantum measurements," Ph.D. thesis, Australian National University (2001).

1. Introduction

Over the past decade, the detectors of the Laser Interferometer Gravitational-wave Observatory (LIGO) have been operating with optical shot noise as the limiting noise source above 150 Hz, which is a large fraction of their total detection band spanning about 50 Hz to 10 kHz [1]. A natural path to improving upon the shot noise limit is to inject appropriately engineered squeezed vacuum states into the output port of interferometers [2–4].

Relative to a vacuum state, a squeezed vacuum state has a smaller variance in one (squeezed) quadrature and a larger variance in the orthogonal (anti-squeezed) quadrature. States with a high degree of squeezing are not only the most promising method available to improve the astrophysical reach of laser interferometer gravitational wave detectors [5–7], they are also an important resource for quantum information and precision measurement. Decoherence limits the utility of highly squeezed states in all these applications. In this letter we show that our theoretical models explain experimental observations of an important decoherence effect: fluctuations of the squeezed quadrature relative to the measured signal quadrature.

Relative fluctuations between the squeezed quadrature and the measured quadrature (also called phase noise or squeezing angle jitter) project noise from the anti-squeezed quadrature into the measurement [8, 9]. When these fluctuations occur faster than the measurement time, they decrease the average level of measured squeezing [10]; when they are slower than the measurement time they limit the long term stability of the measurement. Quadrature stability is especially important in gravitational wave interferometers, where the measurement frequencies may be as low as 10 Hz and long term stability over weeks or months is required.

Optical losses also reduce the squeezing factor by introducing vacuum fluctuations into the squeezed field. While optical losses are the most important limit in many current experiments [5–7, 11, 12], quadrature fluctuations become an increasingly significant limit to the measured squeezing level as the optical losses are reduced.

With a quantum noise limited detector the measurable level of squeezing is [13–15]

$$V_{sqz} = 1 + 4\eta x \left[\frac{\left(\sin\tilde{\theta}\right)^2}{(1-x)^2 + 4(\Omega/\gamma_a^{\text{tot}})^2} - \frac{\left(\cos\tilde{\theta}\right)^2}{(1+x)^2 + 4(\Omega/\gamma_a^{\text{tot}})^2} \right], \tag{1}$$

if the squeezing angle fluctuations have a Gaussian distribution. Here η is the total detection efficiency (the product of the escape efficiency of the optical parametric oscillator (OPO),the propagation, homodyne and photo detector efficiencies); x is the normalized nonlinear coupling ($x = 1 - 1/\sqrt{g}$, where g is the parametric gain); $\tilde{\theta}$ is the root mean squared (RMS) quadrature fluctuation; Ω is the measurement frequency; and γ_a^{tot} is the cavity field decay rate for the squeezed field (the sum of the decay rates for each loss mechanism, $\Sigma\gamma_a^{\text{i}} = (1 - \sqrt{R_{\text{i}}})/\tau$, where τ is the cavity round trip time and R_{i} is a power reflectivity for each loss mechanism). An increase in the nonlinear coupling parameter x increases the amount of both squeezing and anti squeezing generated; in the presence of quadrature fluctuations there is an optimal value of x at which the benefit due to increased squeezing is balanced against the increase in noise introduced by quadrature fluctuations from the anti-squeezed quadrature, as will be seen in Section 4. This means that as long as adequate second harmonic pump power is available and technical noise is negligible, the losses and total quadrature fluctuations in an experiment determine the maximum level of squeezing that can possibly be measured, illustrated in Fig. 1.
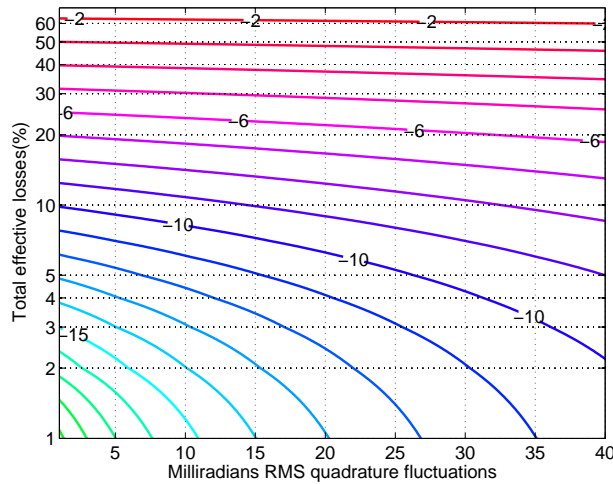
Fig. 1. Possible squeezing as a function of the total effective losses $100 \times (1 - \eta)$ and total squeezed quadrature fluctuations, in the absence of technical noise. Here pump power is optimized for best squeezing given the level of quadrature fluctuations. Squeezing levels in decibels relative to shot noise are negative for an improvement in sensitivity.

A schematic of an experiment in which squeezed vacuum is injected into a LIGO interferometer is shown in Fig. 2 [5, 16]. In this interferometer 20 Watts of 1064 nm laser light is incident on a power-recycled Michelson interferometer with 4 km long Fabry-Perot cavities in each arm. The interferometer optics are suspended from a seismic isolation system inside vacuum to reduce environmental noise coupling. The small amount of light that exits the interferometer at the anti-symmetric port is filtered by an output mode cleaner (OMC) before the gravitational wave signal is read out through self-homodyne detection at the readout photodetectors [17]. Our squeezed light source uses a traveling wave OPO resonant for the second harmonic pump at 532 nm and the fundamental field at 1064 nm [11, 18]. To produce squeezing at the low frequencies required for gravitational wave detection, the OPO is operated with no coherent circulating field at the interferometer carrier frequency [19–22]. A frequency-offset coherent field is used to generate two error signals for controlling the quadrature angle: the coherent field error signal sensed in reflection off the OPO which is fed-back to the phase of the control laser and the quadrature angle error signal sensed at the interferometer's anti-symmetric port which is fed back to the pump laser phase. This squeezed vacuum source was used to improve the sensitivity of this interferometer by -2.1 dB at frequencies above 2 kHz, with some improvement due to squeezing down to 150 Hz, the lowest frequencies at which squeezing has been observed in an interferometer [5].

2. Fluctuations of squeezed quadrature produced by an OPO

For an OPO cavity that is on resonance and phase matched, the squeezed quadrature is determined by the phase of the incident second harmonic pump (θ_B), as illustrated by the red trace in Fig. 3. Any shift in the phase of the second harmonic pump ($\delta\theta_B$) causes a shift of the quadrature angle away from the minimum noise point by $\delta\theta_B/2$, a mechanism that has long been considered a limitation to the level of squeezing [8, 9, 23]. However, small variations in cavity length and crystal temperature also influence the squeezing angle, and are likely more important than pump noise in many experiments. The calculation of the variance of the OPO

output field [24, 25] is expanded in Appendix 1 to include cavity detuning and imperfect phase matching.

A small shift δL in the cavity length away from resonance will detune the fundamental field by $\Delta_a = \omega \delta L / \overline{L}$ where $\overline{L}$ is the cavity length on resonance and ω is the laser frequency. The second harmonic field will also have a detuning, $\Delta_b = 2\Delta_a$. Fig. 3 shows that the effect of OPO cavity length offsets on the output field variance is well approximated as shift of the pump phase, meaning that it is well described as a shift of the squeezed quadrature. Because the cavity length fluctuations will be at frequencies small compared to the cavity linewidths, we can use this static dependence to approximate the level of quadrature fluctuations caused by cavity length fluctuations. By taking derivatives around a point where the variance (V) has a linear dependence on the pump phase ($\theta_B = \pi/2$ is chosen for convenience), we can find the first order squeezing angle shift ($d\theta_{sqz}$) caused by a cavity length change,

$$\frac{d\theta_{\text{sqz}}}{d\delta L} = \frac{1}{2} \frac{dV/d\delta L}{dV/d\theta_b}\bigg|_{\theta_B = \pi/2, \delta L = 0} = \frac{\omega}{\overline{L}}\left(\frac{1}{\gamma_b^{\text{tot}}} + \frac{1}{\gamma_a^{\text{tot}}(1+x^2)}\right). \tag{2}$$

For our OPO, operated with a nonlinear gain of 10, this gives a coupling of 90 ± 4 mrad squeezed quadrature rotation per nanometer cavity length change. Cavity length fluctuations that occur above the 10 kHz bandwidth of the quadrature control loop directly couple to quadrature fluctuations in this way.
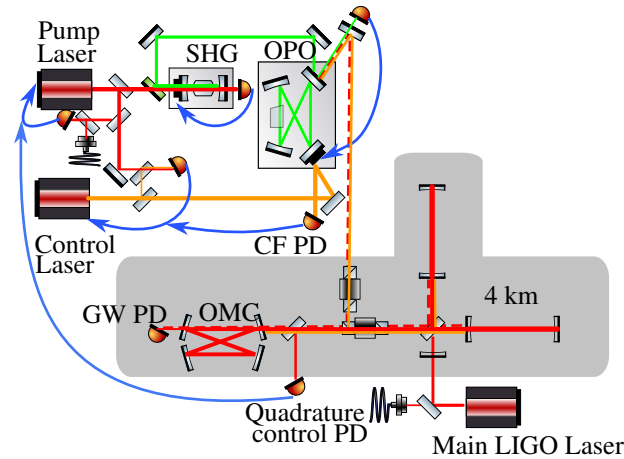

Fig. 2. The LIGO interferometer with a squeezed vacuum source. The pump laser, locked to the LIGO main laser frequency through an optical fiber, pumps the second harmonic generator (SHG) [19] and the optical parametric oscillator (OPO) [18]. The control laser – for the quadrature control scheme – is offset locked 29.5 MHz above the pump laser frequency, and injected into the OPO where the nonlinear interaction generates a symmetric sideband 29.5 MHz below the pump with, under ideal conditions, a phase determined by the phase of the circulating pump [19, 20]. The phase of the control laser is then locked relative to the phase of the circulating pump by the coherent field photo-detector (CF PD). The squeezed field, with coherent control sidebands, reflects off the interferometer after which the quadrature control photo-detector senses the phase between the interferometer beam and the coherent sidebands. This error signal is used to adjust the pump laser phase and control the quadrature angle. The output mode cleaner (OMC) reflects the coherent sidebands and transmits the carrier towards the gravitational wave readout photo-detectors (GW PD) where the squeezing is measured.
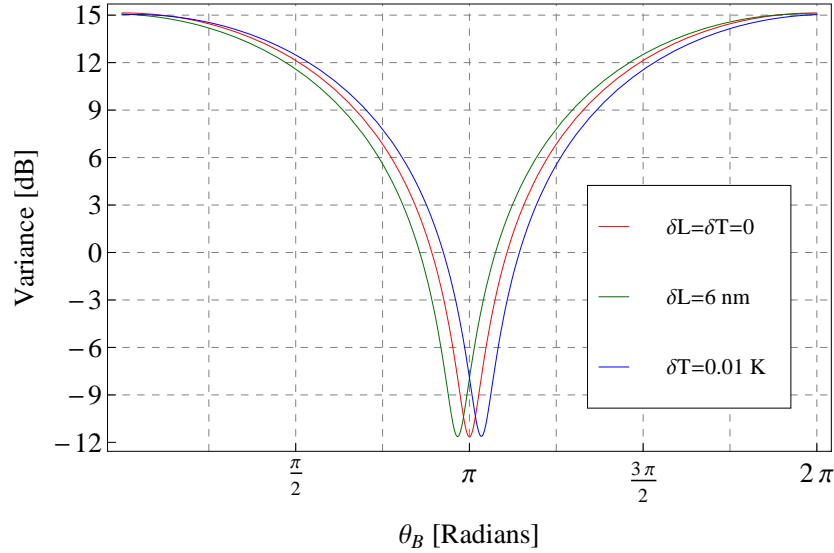
Fig. 3. Variance (in dB relative to vacuum fluctuations) in one quadrature of the OPO output field as a function of the phase of the incident second harmonic pump. With no detuning and ideal phase matching (red trace), the minimum variance occurs at $\theta_B = \pi$, and the pump phase alone determines the squeezed quadrature $\theta_{sqz} = \theta_B/2$. However small changes in the cavity length or crystal temperature shift the location of the minimum variance, introducing a relative shift between the squeezed quadrature angle and the pump phase. The green trace shows the variance with the cavity length shifted 6 nm away from resonance, while the blue trace shows the variance produced when the temperature deviates by 0.01 K from the phase matching temperature. These predictions assume $\Omega \ll \gamma_a^{\text{tot}}, |x| = 1/\sqrt{2}, \eta_{esc} = 0.96$, $\gamma_a^{\text{tot}} = 2\pi \times 12$ MHz, and $\gamma_b^{\text{tot}} = 2\pi \times 30$ MHz.

Inside the bandwidth of the coherent quadrature control loop, the response of the control signal needs to be taken into account to understand the impact of cavity length fluctuations on the squeezed quadrature. The phase shift induced by a cavity length change is smaller for the detuned coherent control field than it is for the squeezed field which is on resonance. This means that the response of the coherent control scheme is smaller than the response of the quadrature angle to cavity length changes, 47 ± 2 mrad/nm for our parameters, as can be calculated using Eqs. (20) and (21) from Appendix 2. The difference in the response of the quadrature control sensor from the response of the quadrature angle introduces lock point errors to the control scheme when cavity length fluctuations are present. Inside the control bandwidth this difference between the response of the actual quadrature angle and the response of the quadrature control error signal (43 ± 4 mrad/nm for our parameters) gives the coupling of cavity length fluctuations to the quadrature angle. Based on our measurements of the cavity length fluctuations we expect 24.6 ± 3 mrad of squeezed quadrature fluctuations below 100 kHz due to cavity length fluctuations, one of the dominant causes of quadrature fluctuations in our experiment.

Fluctuations in the circulating pump power will cause fluctuations in the temperature of the nonlinear crystal due to absorption. Changes in the crystal temperature in turn cause a phase mismatch, and change the resonance condition of the cavity due to thermal expansion and a change in the refractive index of the crystal [26,27]. For imperfect phase matching the nonlinear

coupling parameter becomes [28]

$$\varepsilon = \varepsilon_0 e^{-i\kappa(T-T_0)} \operatorname{sinc}\left(\kappa(T-T_0)\right). \tag{3}$$

where ε_0 is the nonlinear coupling parameter at the phase matching temperature, T_0 is the phase matching temperature, and κ is a constant that depends on the phase matching type and crystal used (0.579/K for quasi phase matching in PPKTP as used in this experiment). A change in temperature will also cause a shift in the cavity resonance condition, the more important effect in our case. To produce audio frequency squeezing the field used to lock the length of an OPO must be either the second harmonic [11, 18] or a polarization shifted field offset from the fundamental frequency [19, 20]. In either case, the resonance condition of the field used for length locking is manually adjusted to coincide with the resonance of the fundamental field and a change in crystal temperature will shift the two cavity modes away from co-resonance. The length of the OPO in this experiment was locked to the second harmonic field, so the detuning of the fundamental field due to a temperature change is

$$\Delta_a = -\kappa(T-T_0)/\tau, \tag{4}$$

where τ is the cavity round trip time. Taking both of these effects into account, the variance as a function of the input pump phase can be found using Eqs. (11), (13), and (14), and is plotted as the blue curve in Fig. 3. Again taking derivatives around $\theta_B = \pi/2$ we can find the linear shift in the squeezed quadrature angle caused by a temperature change:

$$\frac{d\theta_{\text{sqz}}}{dT} = \frac{1}{2} \frac{dV/dT}{dV/d\theta_b}\bigg|_{\theta_B=\pi/2, T=T_0} = -\kappa\left(\frac{1}{\gamma_a^{\text{tot}}\tau(1+x^2)} + \frac{1}{2}\right). \tag{5}$$

Similar to cavity length fluctuations, crystal temperature fluctuations cause lock point errors in the quadrature control error signal. Although a temperature shift of 1 mK would cause the squeezing angle to shift 5.5 ± 0.6 mrad for our parameters (Eq. (5)), the coherent quadrature control sensor will only sense 1.5 ± 0.2 mrad/mK based on the calculation in Appendix 2 (Eqs. (21) and (20)). Since temperature fluctuations are at frequencies well inside the coherent control bandwidth, we predict that temperature fluctuations will cause squeezing angle fluctuations of 4 ± 0.6 mrad/mK. A measurement confirmed that the lock point had to be shifted 4.6 ± 0.5 mrad/mK to reoptimize the measured squeezing after a temperature change. With 50 mW second harmonic input power incident on our OPO the crystal temperature increased by approximately 6.9 mK/mW increase in the pump power. The pump power drifts of less than 1% observed on half hour time scales would produce a squeezing angle shift of $5 \pm 1 mrad$, too small to be significant in our experiment. Over 60 hours, our pump power fluctuated by 5%, enough to cause degradation of the measured squeezing as seen in [27]. The total temperature fluctuations in the crystal are unknown, and caused by a combination of and pump power fluctuations, environmental temperature changes, and noise of the temperature sensor used for stabilization.

3. Relative quadrature fluctuations introduced by measurement and control schemes

The squeezed quadrature rotates as the field propagates from the OPO output coupler to the detector with a rotation equivalent to the phase shift a coherent field would experience propagating along the same path, so path length changes directly couple to relative quadrature fluctuations. In interferometers squeezing is measured using unbalanced homodyne detection, with the local oscillator provided by the interferometer output beam which is filtered by the OMC. This local oscillator is made up of the interferometer signal field, and a small amount of other light due to contrast defect and the interferometer control sidebands. The quadrature of the squeezed

beam that is measured is determined by the relative phase of the local oscillator, so local oscillator phase noise directly causes quadrature fluctuations unless it is suppressed by the control scheme.

Modulation sidebands at frequencies well above the quadrature control bandwidth are used to control interferometer length and alignment degrees of freedom, adding phase noise to the local oscillator. In LIGO an optical cavity at the anti-symmetric port, the OMC, is used to filter amplitude and phase noise at frequencies above a few MHz. The sidebands that do reach the output photodetector are in the amplitude quadrature of the interferometer signal field, however there are two mechanisms by which these modulation sidebands can modulate the phase of the local oscillator. If the two sidebands are not exactly the same in size, the total modulation will be described as amplitude modulation with a small component of phase modulation. Likewise, a small contrast defect field at the carrier frequency which arrives at the anti-symmetric port out of phase with the interferometer signal field will shift the phase of the total local oscillator at the anti-symmetric port, and therefore a small amount of the amplitude noise on the interferometer signal field will become phase modulation on the total local oscillator. The total radio frequency phase modulation of the local oscillator is the quadrature sum of these two out-of-phase contributions,

$$\tilde{\theta}_{\mathrm{RF}} = \sqrt{\frac{T_{\mathrm{SB}}}{P_{\mathrm{sig}}} \left(\frac{2\bar{P}_{\mathrm{SB}} P_{\mathrm{CD}}}{P_{\mathrm{sig}}} + \frac{dP_{\mathrm{SB}}^2}{8\bar{P}_{\mathrm{SB}}} \right)},$$ (6)

where T_{SB} is the power transmission of the sidebands through the OMC, $\bar{P}_{\mathrm{SB}}$ is the average power in each sideband, dP_{SB} is the difference between the sidebands powers, P_{CD} is the power of the contrast defect field, and P_{sig} is the power in the signal field. The squeezing angle jitter added by this modulation is small in our case due to the excellent filtering provided by the OMC, and only contributes 3.1 ± 0.4 mrad.

The control scheme described in Fig. 2 compensates for path length changes and local oscillator phase noise within its bandwidth. The control scheme can also impose noise from the sensors used onto the squeezing angle fluctuations. Based on measurement of the sensor noise and the feedback response we project the sensor noise imposes less than 2 mrad of squeezed quadrature in our experiment. If this noise source were a dominant effect, the level of squeezing angle fluctuations measured would increase when the gain of the control system is increased.

4. Measurements of relative quadrature fluctuations

The total RMS quadrature fluctuations as well as the total detection efficiency in a squeezing experiment can be inferred from measurements of squeezing and anti-squeezing made at high nonlinear gains, as shown in Fig. 4. Because the couplings of both temperature and length fluctuations decrease at high nonlinear gains, this method can lead to a small underestimation of the total quadrature fluctuations. This can be accounted for using Eqs. (2) or (5) if the dominant noise mechanism is known. In our experiment, measurements made with nonlinear gains of up to $g = 100$ on a balanced homodyne detector showed that the total quadrature fluctuations intrinsic to the squeezed state source were 18.6 ± 5.7 mrad before injection into the interferometer, consistent with the level of squeezed quadrature fluctuations we predict based on OPO length noise. Assuming that length fluctuations are the dominant source of quadrature angle errors, we can infer from our high nonlinear gain measurements that the RMS quadrature fluctuations will be 21 ± 6 mrad when the nonlinear gain is 10, the normal operating point.

A similar measurement was performed with the interferometer, as shown in Fig. 5, revealing larger than expected quadrature fluctuations. This excess noise is caused by lock point errors introduced by angular misalignment between the interferometer output beam and the squeezed
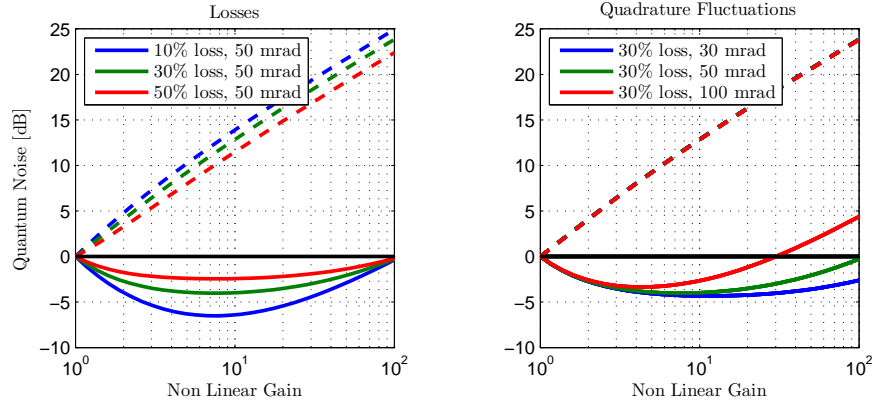
Fig. 4. Expected variances of the squeezed (solid lines) and anti-squeezed (dashed lines) quadratures as a function of nonlinear gain, based on Eq. (1). The level of anti-squeezing is sensitive to the total losses, while at high gains the level of squeezing is sensitive to the quadrature fluctuations. Left panel: $\tilde{\theta}$ =50 mrad and η= 90% (blue) 70% (green) and 50% (red). Right panel: η=70%, and $\tilde{\theta}$=30 (blue), 50 (green), and 100 (red) mrad. Blue and green dashed lines are below the red dashed line in the right panel.

beam. At the quadrature control photo-detector both the local oscillator beam and the squeezed beam include higher-order spatial modes that contribute to the error signal with a different phase than the TEM$_{00}$ mode because of the Gouy phase shift. This means that relative alignment shifts change the lock point of the coherent locking loop, and alignment jitter couples to quadrature fluctuations. A change in alignment will shift the relative quadrature angle by an amount:

$$\Delta\theta_{\text{alignment}} = -\frac{\Sigma_{ij}\gamma_{ij}^{\text{ifo}}\gamma_{ij}^{\text{clf}}\sin\phi_{ij}}{1-\Sigma_{ij}\gamma_{ij}^{\text{ifo}}\gamma_{ij}^{\text{clf}}\cos\phi_{ij}}, \tag{7}$$

where $\gamma_{ij}^{\text{ifo}}, \gamma_{ij}^{\text{clf}}$ are the ratio of the amplitudes of the ij spatial modes to th amplitude of the 00 mode for the interferometer field and the coherent quadrature control field respectively, and ϕ_{ij} is the difference between the relative phases of the ij modes and the relative phases of TEM$_{00}$ modes of the two beams. This coupling becomes second-order when the two beams are well aligned, as shown by the reduced quadrature fluctuations measured by the green point in Fig. 5 using a finely tuned alignment.

One can measure the spectrum of quadrature fluctuations directly by setting the squeezing angle so that the measured noise level has a linear dependence on the squeezing angle. Measuring a time series of the noise power in a shot noise limited frequency band provides an out of loop measurement of the quadrature fluctuations. A measurement of this type, compared to the quadrature control error signal and sensor noise from the quadrature control sensor confirmed that the coherent quadrature sensor has lock point errors from 0.1 Hz to 10 Hz, consistent with the frequencies of alignment jitter in the interferometer.

5. Implications for future gravitational wave detectors with squeezing

As shown in Fig. 6, we measured just over -2 dB of squeezing in Enhanced LIGO with 55% losses and at least 37 ± 6 mrad quadrature fluctuations. Table 1 summarizes the mechanisms
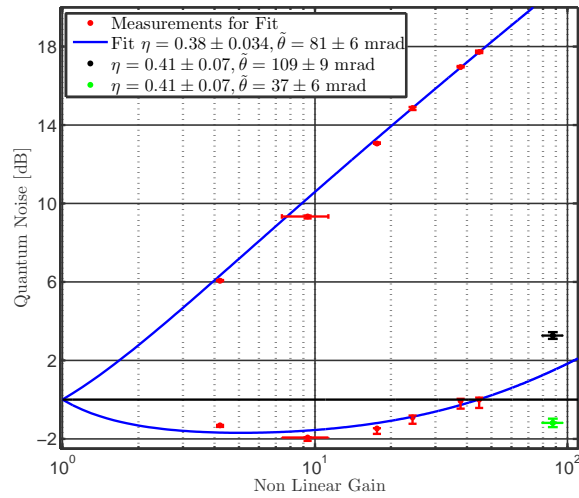
Fig. 5. Characterization of Enhanced LIGO interferometer as a squeezing detector. Red points show measured squeezing and anti squeezing between 1.9 kHz and 3.7 kHz. Blue trace is a fit to the red points with $\eta = 38 \pm 3\%$ and $\tilde{\theta} = 81 \pm 6$ mrad. Control bandwidths were consistent for measurements at different nonlinear gains. The black and green points were measured at a later date with $\eta = 42 \pm 7\%$. After measurement of the black point ($\tilde{\theta} = 109 \pm 9$ mrad), the interferometer alignment was adjusted slightly and the squeezing angle lock point adjusted, reducing the quadrature fluctuations to ($\tilde{\theta} = 37 \pm 6$ mrad) as shown by the green point.

Table 1. Summary of contributions to total relative quadrature fluctuations (mrad RMS) and independent measurements made at high nonlinear gains.

	Source	Estimate	Measurement
Squeezer	OPO length noise	24.6 ± 3	
	Coherent locking field(CLF) sensor noise	1.8 ± 0.5	
	OPO and SHG length control sidebands	< 1	
	Crystal temperature fluctuations	unknown	
	Total intrinsic to squeezer	24.7 ± 2	21 ± 6
IFO	Interferometer (IFO) sidebands	3.1 ± 0.4	
	Alignment jitter coupling (inferred from total)	35-100	
	Squeezer + IFO total (good alignment)		37 ± 6

considered here that cause quadrature fluctuations, and our estimates and measurements of their contribution to the total in our experiment. The dominant mechanism for relative fluctuations between the squeezed and measured quadrature in our experiment was lock point errors introduced by alignment fluctuations, closely followed by length fluctuations of the OPO. Other smaller contributions were phase noise of the second harmonic pump, temperature fluctuations, sensor electronics and shot noise imposed by our control scheme, and phase noise of the local oscillator.

In the early stages of Advanced LIGO [29], the total effective losses are expected to be reduced to 20-28%, mainly due to improvements in OMC transmission and mode matching. This means that a reduction of the quadrature fluctuations to 5-15 mrad would allow for confident
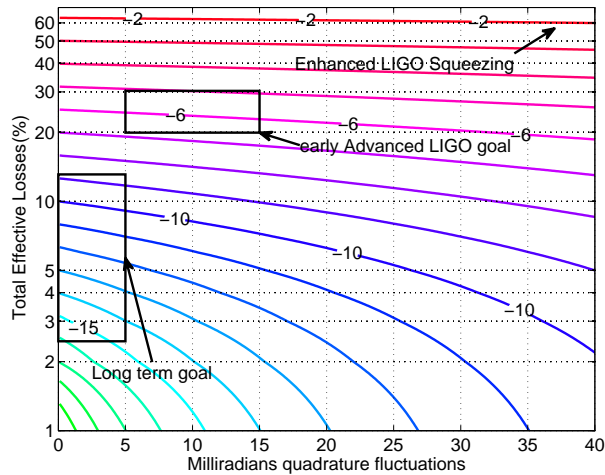
Fig. 6. Squeezing targets for gravitational wave detectors, in decibels relative to shot noise. This experiment measured -2.1 dB of squeezing in Enhanced LIGO, with 55% losses and at least 37 ± 6 mrad squeezing angle fluctuations. For Advanced LIGO we would like to be able to measure at least -6 dB of squeezing in an initial implementation. Since the total losses are expected to be 20-28%, planning for 15 mrad or less of phase noise would allow for -6 dB of squeezing. Designs for third generation detectors call for even higher levels of squeezing [31], which will place very stringent limits on the total quadrature fluctuations and losses.

planning for -6 dB of noise reduction due to squeezing, as shown by the rectangle in Fig. 6. These levels of quadrature fluctuations have already been demonstrated with both traveling wave and standing wave OPO designs [11, 30]. Third generation detectors seek to implement 10 dB or more of squeezing [31], placing very stringent requirements on both optical losses and quadrature fluctuations.

The performance of the coherent quadrature control schemes is limited by lock point errors introduced by alignment jitter, OPO length fluctuations, and crystal temperature fluctuations. The bandwidth of the coherent control scheme is limited by arm cavity resonances in an interferometer with Fabry-Perot arms; in LIGO this limits the bandwidth to around 10 kHz. Quantum noise locking [32] is an alternative to coherent locking that is immune to lock point errors and could potentially reduce the quadrature fluctuations to a comfortable level for Advanced LIGO when used in combination with a coherent lock [7]. However, the dither of the quadrature angle required to produce a noise locking error signal will need to be small compared to the acceptable level of quadrature fluctuations, meaning that this technique will have a small signal to noise ratio and therefore low bandwidth. Ultimately, to achieve the low levels of quadrature fluctuations needed, the lock point errors of the coherent control scheme need to be addressed.

One option is to derive the coherent control error signal in transmission of the OMC [7], which should eliminate the alignment coupling to the quadrature angle by filtering the higher order modes. The OPO may be mounted on a seismic isolation platform inside the vacuum system in order to meet the requirements for scattered light noise. This will have the benefit of reducing both the length fluctuations of the OPO and relative alignment fluctuations between the OPO and the interferometer, mitigating both of the dominant sources of quadrature fluctuations in this experiment. Intensity stabilization of the second harmonic pump [27], or a direct readout of the crystal temperature similar to the scheme used in [26], may help to mitigate lock

point errors caused by crystal temperature fluctuations.

We have shown that careful attention must be paid to each of the major causes of quadrature fluctuations in order to reach high levels of squeezing enhancement in a gravitational wave interferometer, or any experiment where high levels of squeezing are needed. The low frequency noise requirements of a gravitational wave detector preclude use of a coherent field at the carrier frequency for sensing and control of the quadrature angle, making it necessary to use either incoherent "noise" locking or coherent control schemes with a frequency-shifted sideband. Both of these techniques have limitations: the coherent locking technique introduces lock point errors due to misalignment, OPO length changes and crystal temperature fluctuations, while noise locking relies on a dither of the quadrature angle. Ultimately, quadrature fluctuations need to be mitigated at the source rather than suppressed by high bandwidth feedback. This requires careful planning and an understanding of each of the sources of quadrature fluctuations.

6. Appendix 1: Calculation of squeezed quadrature angle in an OPO including detunings and imperfect phase matching

The Hamiltonian for an OPO without losses is:

$$H = \hbar 2\omega b^\dagger b + \hbar \omega a^\dagger a + \frac{i\hbar}{2}(\varepsilon a^{\dagger 2} b + \varepsilon^* a^2 b^\dagger) \tag{8}$$

where $a, a^\dagger$ are annihilation and creation operators for the fundamental field at the interferometer carrier frequency ω written in the rotating frame at that frequency, $b, b^\dagger$ are operators for the second harmonic field in the rotating frame at 2ω, and ε is the nonlinear coupling parameter which is real when the crystal temperature is exactly tuned for phase matching. We can calculate the spectrum of squeezing at the output of the OPO using the quantum Langevin equations and introducing two losses to the cavity, one representing all of the intracavity losses and absorption and another representing transmission through the front coupler [24, 25]. The steady state solution to the cavity equation of motion for the second harmonic field in the parametric approximation is:

$$b = \frac{\sqrt{2\gamma_b^f}|B_{in}|}{\gamma_b^{tot}} \frac{e^{i\theta_B}}{1 - i\Delta_b/\gamma_b^{tot}} \tag{9}$$

where $B_{in} = |B_{in}|e^{i\theta_B}$ is the incident second harmonic pump field in the rotating frame at 2ω, γ_b^f is the field decay rate of the front coupler for the second harmonic field, γ_b^{tot} is the total field cavity decay rate for the second harmonic field, and Δ_b is a detuning of the second harmonic field from the cavity resonance. The operators can be separated into constant and time dependent parts, $(a = \bar{a} + \delta a(t), b = \bar{b} + \delta b(t))$, and the equations of motion for the fundamental field linearized by dropping terms that are the product of two fluctuating components. To avoid noise couplings that mask low frequency squeezing, there should be no circulating coherent field at the fundamental frequency so $\bar{a} = 0$ [22]. The equations of motion for the fundamental field annihilation and creation operators are given in matrix form by:

$$\delta \dot{\mathbf{a}} = \gamma_a^{tot} \mathbf{M} \delta \mathbf{a} + \sqrt{2\gamma_a^l}\delta \mathbf{A}_{l,in} + \sqrt{2\gamma_a^f}\delta \mathbf{A}_{f,in} \tag{10}$$

where

$$\delta \mathbf{a} = \begin{pmatrix} \delta a \\ \delta a^\dagger \end{pmatrix}, \quad \mathbf{M} = \begin{pmatrix} -1 + i\dfrac{\Delta_a}{\gamma_a^{tot}} & x\dfrac{e^{i\theta_B}}{1 - i\Delta_b/\gamma_b^{tot}} \\ x^*\dfrac{e^{-i\theta_B}}{1 + i\Delta_b/\gamma_b^{tot}} & -1 - i\dfrac{\Delta_a}{\gamma_a^{tot}} \end{pmatrix}, \quad x = \frac{\sqrt{2\gamma_b^f}|B_{in}|}{\gamma_b^{tot}}\frac{\varepsilon}{\gamma_a^{tot}} \tag{11}$$

and $\delta\mathbf{A}_{\mathrm{l,in}}$ is a vector of the annihilation and creation operator for the vacuum fluctuations that leak into the cavity through intra-cavity losses and $\delta\mathbf{A}_{\mathrm{f,in}}$ are the vacuum fluctuations incident on the front coupler of the OPO, $\gamma_a^{\mathrm{tot}} = \gamma_a^{\mathrm{l}} + \gamma_a^{\mathrm{f}}$ is the total cavity field decay rate for the fundamental field, γ_a^{f} is the decay rate for the front coupler for the fundamental field, γ_a^{l} is the decay rate due to intracavity losses, and Δ_a is the cavity detuning at the fundamental frequency. The normalized nonlinear coupling x is real when the temperature is tuned to phase matching, and reaches unity when the OPO reaches the threshold for spontaneous parametric down conversion. Moving into the frequency domain:

$$\delta\widetilde{\mathbf{a}}(\Omega) \quad = (\Omega - \gamma_a^{\mathrm{tot}}\mathbf{M})^{-1} \left[\sqrt{2\gamma_a^{\mathrm{l}}}\delta\widetilde{\mathbf{A}}_{\mathrm{l,in}}(\Omega) + \sqrt{2\gamma_a^{\mathrm{f}}}\delta\widetilde{\mathbf{A}}_{\mathrm{f,in}}(\Omega) \right] \tag{12}$$

Here we have assumed that $\mathbf{M}$ does not depend on time, which is a good approximation when the time dependence is at frequencies much smaller than the cavity linewidths $\gamma_b^{\mathrm{tot}}, \gamma_a^{\mathrm{tot}}$, as temperature and length fluctuations will be. Using the input output relations [24]:

$$\delta\mathbf{A}_{\mathrm{f,out}}(\Omega) \quad = \sqrt{2\gamma_a^{\mathrm{f}}}\delta\widetilde{\mathbf{a}}(\Omega) - \delta\widetilde{\mathbf{A}}_{\mathrm{f,in}}(\Omega) \tag{13}$$

$$= \left(2\gamma_a^{\mathrm{f}} \left(i\Omega\mathbf{I} - \gamma_a^{\mathrm{tot}}\mathbf{M} \right)^{-1} - \mathbf{I} \right) \delta\mathbf{A}_{\mathrm{f,in}}(\Omega) + 2\sqrt{\gamma_a^{\mathrm{l}}\gamma_a^{\mathrm{f}}} \left(i\Omega\mathbf{I} - \gamma_a^{\mathrm{tot}}\mathbf{M} \right)^{-1} \delta\mathbf{A}_{\mathrm{l,in}}(\Omega)$$

When the measurement frequency Ω is small compared to the optical frequency ω, the quadrature operators of the output field are given in terms of the annihilation and creation operators by [33]:

$$\delta\widetilde{\mathbf{X}}_{\mathrm{f,out}}(\Omega) = \left(\begin{array}{c} \delta\widetilde{X}_1(\Omega) \\ \delta\widetilde{X}_2(\Omega) \end{array} \right) = \left(\begin{array}{cc} 1 & 1 \\ -i & i \end{array} \right) \delta\widetilde{\mathbf{A}}_{\mathrm{f,out}}(\Omega) = \mathbf{R}\delta\widetilde{\mathbf{A}}_{\mathrm{f,out}}(\Omega) \tag{14}$$

Using the fact that the incident vacuum fluctuations are uncorrelated [34], the variance of the output field ($V_1 = |\delta\widetilde{X}_1|^2$) can be calculated using Eqs. (11), (13), and (14); results are plotted in Fig. 3. The usual equations for the variance of the output field can be found by setting the detunings Δ_a, Δ_b to zero, assuming that ε is real:

$$V_1(\theta_b, \Omega) \quad = V_+(\Omega)\cos^2(\theta_b/2) + V_-(\Omega)\sin^2(\theta_b/2)$$

$$V_\pm \quad = 1 \pm \frac{4\eta_{\mathrm{esc}}x}{(1 \mp x)^2 + (\Omega/\gamma_a^{\mathrm{tot}})^2} \tag{15}$$

where $\eta_{\mathrm{esc}} = \gamma_a^{\mathrm{f}}/\gamma_a^{\mathrm{tot}}$ is the escape efficiency. By propagating this field to the detector and taking into account additional loses in propagation, homodyne efficiency and photo-diode efficiency, Eq. (1) is obtained.

7. Appendix 2: Calculation of control signals including detunings and imperfect phase matching

To calculate the error signal produced by the coherent locking technique, we can use the cavity equations of motion for a non-degenerate OPO, approximating the two coherent control sidebands as separate modes of the cavity, called the signal (a_{s}) and idler (a_{i}). Assuming that the signal and idler fields are small compared to the second harmonic field the parametric approximation holds and the second harmonic field is described by Eq. (9). Ignoring quantum fluctuations, the equations of motion are:

$$\dot{a}_{\mathrm{s}} = (i\Delta_{\mathrm{s}} - \gamma_a^{\mathrm{tot}})a_{\mathrm{s}} + \varepsilon b a_{\mathrm{i}}^\dagger + \sqrt{2\gamma_a^{\mathrm{c}}}A_{\mathrm{s,in}} \tag{16}$$

$$\dot{a}_{\mathrm{i}} = (i\Delta_{\mathrm{i}} - \gamma_a^{\mathrm{tot}})a_{\mathrm{i}} + \varepsilon b a_{\mathrm{s}}^\dagger \tag{17}$$

and their hermitian conjugates, where $\Delta_s = \Delta_a + \Omega_{\text{offs}}$ and $\Delta_i = \Delta_a - \Omega_{\text{offs}}$ are the detunings of the signal and idler fields when the frequency offset of the injected field from the fundamental frequency is Ω_{offs}. Because the control bandwidth is small compared to the cavity linewidth, we find the response of the error signals to a static change by setting the derivatives to zero and solving the set of equations. The input output relations can be used to find the coherent control fields in reflection off the OPO, $A_{s,r}, A_{i,r}$ and transmitted towards the interferometer, $A_{s,t}, A_{i,t}$:

$$A_{s,r} = \sqrt{2\gamma_a^c}\, a_s - A_{s,\text{in}} \qquad\qquad A_{i,r} = \sqrt{2\gamma_a^c}\, a_i \qquad\qquad (18)$$

$$A_{s,t} = \sqrt{2\gamma_a^f}\, a_s \qquad\qquad\qquad A_{i,t} = \sqrt{2\gamma_a^f}\, a_i \qquad\qquad (19)$$

The error signal in reflection off of the cavity (demodulated at twice the frequency offset of the injected field from the interferometer with a demodulation phase ϕ_{dm1} is proportional to:

$$E_r = \text{Re}[A_{s,r} A_{i,r}^{\dagger}] \sin\phi_{\text{dm1}} + \text{Im}[A_{s,r} A_{i,r}^{\dagger}] \cos\phi_{\text{dm1}} \qquad\qquad (20)$$

In transmission the beat note with the local oscillator (A_{LO}) is demodulated at the offset frequency with a demodulation phase ϕ_{dm2} to give a signal proportional to:

$$E_t = \text{Re}[A_{s,t} A_{\text{LO}}^{\dagger} + A_{i,t}^{\dagger} A_{\text{LO}}] \sin\phi_{\text{dm2}} + \text{Im}[A_{s,t} A_{\text{LO}}^{\dagger} + A_{i,t}^{\dagger} A_{\text{LO}}] \cos\phi_{\text{dm1}} \qquad\qquad (21)$$

The relative phase between the main squeezing laser and the coherent sideband injected into the OPO is adjusted to zero the reflected (coherent field) error signal, so the impact of fluctuations can be found by setting the error signal to zero and solving numerically for change in the phase of $A_{s,in}$. This phase is then propagated to the transmitted (quadrature control) error signal, and the shift of the pump phase required to zero this error signal gives the response of the entire coherent quadrature control scheme to a disturbance. The response of this scheme is the same as the response of the quadrature angle itself to fluctuations of the second harmonic pump phase, local oscillator phase, or path length from the OPO to the detector; this is a good control scheme to use to correct for fluctuations from those sources. Temperature and length fluctuations give rise to lock point errors in this control scheme.